

THE AAA ALGORITHM FOR RATIONAL APPROXIMATION

YUJI NAKATSUKASA*, OLIVIER SÈTE†, AND LLOYD N. TREFETHEN‡

For Jean-Paul Berrut, the pioneer of numerical algorithms based on rational barycentric representations, on his 65th birthday.

Abstract. We introduce a new algorithm for approximation by rational functions on a real interval or a set in the complex plane, implementable in 40 lines of Matlab. Even on a disk or interval the algorithm may outperform existing methods, and on more complicated domains it is especially competitive. The core ideas are (1) representation of the rational approximant in barycentric form with interpolation at certain support points, (2) greedy selection of the support points to avoid exponential instabilities, and (3) least-squares rather than interpolatory formulation of the overall problem. The name AAA stands for “aggressive Antoulas–Anderson” in honor of the authors who introduced a scheme based on (1). We present the core algorithm with a Matlab code and eight applications and describe variants targeted at problems of different kinds.

Key words. rational approximation, barycentric formula, analytic continuation, AAA algorithm, Froissart doublet

AMS subject classifications. 41A20, 65D15

1. Introduction. Rational approximations of real or complex functions are used mainly in two kinds of applications. Sometimes they provide compact representations of functions, much more efficient than polynomials for functions with poles or other singularities on or near the domain of approximation or on unbounded domains. Other times, their role is one of extrapolation: the extraction of information about poles or values or other properties of a function in regions of the real line or complex plane beyond where it is known a priori. For example, standard methods of acceleration of convergence of sequences and series, such as the eta and epsilon algorithms, are based on rational approximations [6, 15]. For a general discussion of the uses of rational approximation, see Chapter 23 of [38], and for theoretical foundations, see [14].

Working with rational approximations, however, can be problematic. There are various challenges here, one of which particularly grabs attention: *spurious poles*, also known as *Froissart doublets*, which can be regarded either as poles with very small residues or as pole-zero pairs so close together as to nearly cancel [19, 37]. Froissart doublets arise in the fundamental mathematical problem — i.e., in “exact arithmetic” — and are the reason why theorems on convergence of rational approximations, e.g. of Padé approximants along diagonals of the Padé table, typically cannot hold without the qualification of convergence in capacity rather than uniform convergence [6, 31]. On a computer in floating point arithmetic, they arise all the more often; we speak of *numerical Froissart doublets*, recognizable by residues on the order of machine precision. These difficulties are related to the fact that the problem of analytic con-

*nakatsukasa@maths.ox.ac.uk, Mathematical Institute, University of Oxford, Oxford, OX2 6GG, UK.

†sete@maths.ox.ac.uk, Mathematical Institute, University of Oxford, Oxford, OX2 6GG, UK.

‡trefethen@maths.ox.ac.uk, Mathematical Institute, University of Oxford, Oxford, OX2 6GG, UK. YN was supported by the Japan Society for the Promotion of Science as a Postdoctoral Fellow for Research Abroad. OS and LNT were supported by the European Research Council under the European Union’s Seventh Framework Programme (FP7/2007–2013)/ERC grant agreement 291068. The views expressed in this article are not those of the ERC or the European Commission, and the European Union is not liable for any use that may be made of the information contained here.

tinuation, for which rational approximation is the most powerful general technique, is ill-posed. See Chapter 26 of [38].

In this paper we propose a *AAA algorithm* for rational approximation that offers a speed, flexibility, and robustness we have not seen in other algorithms; the name stands for “aggressive Antoulas–Anderson”¹. The algorithm combines three ideas. First, following Antoulas and Anderson [2] (though their presentation of the mathematics is very different), rational functions are represented in barycentric form with interpolation at certain support points selected from a set provided by the user. (Related methods appear in [9] and [11].) Second, the algorithm grows the approximation degree one by one, selecting support points in a systematic greedy fashion so as to avoid exponential instabilities. Third, the algebra is set in the mode of linearized least-squares fitting rather than just interpolation, further enhancing robustness and making it extensible to continuous as well as discrete domains. Numerical Froissart doublets usually do not appear, and if they do, they can be removed by one further solution of a least-squares problem.

2. Rational barycentric representations. The barycentric formula takes the form of a quotient of two partial fractions,

$$(2.1) \quad r(z) = \frac{n(z)}{d(z)} = \sum_{j=1}^m \frac{w_j f_j}{z - z_j} \bigg/ \sum_{j=1}^m \frac{w_j}{z - z_j},$$

where $m \geq 1$ is an integer, z_1, \dots, z_m are a set of real or complex distinct *support points*, f_1, \dots, f_m are a set of real or complex *data values*, and w_1, \dots, w_m are a set of real or complex *weights*. As indicated in the equation, we let $n(z)$ and $d(z)$ stand for the partial fractions in the numerator and the denominator. When we wish to be explicit about step numbers, we write $r_m(z) = n_m(z)/d_m(z)$.

The *node polynomial* ℓ associated with the set z_1, \dots, z_m is the monic polynomial of degree m with these numbers as roots,

$$(2.2) \quad \ell(z) = \prod_{j=1}^m (z - z_j).$$

If we define

$$(2.3) \quad p(z) = \ell(z)n(z), \quad q(z) = \ell(z)d(z),$$

then p and q are each polynomials of degree at most $m - 1$. Thus we have a simple link between the barycentric representation of r and its more familiar representation as a quotient of polynomials,

$$(2.4) \quad r(z) = \frac{p(z)/\ell(z)}{q(z)/\ell(z)} = \frac{p(z)}{q(z)}.$$

This equation tells us that r is a rational function of type $(m - 1, m - 1)$, where, following standard terminology, we say that a rational function is of *type* (μ, ν) for integers $\mu, \nu \geq 0$ if it can be written as a quotient of a polynomial of degree at most μ and a polynomial of degree at most ν , not necessarily in lowest terms.² The numerator

¹We write “a AAA” rather than “an AAA” because in speech we say “triple-A.”

²As a special case it is also customary to say that the zero function is not only of type (μ, ν) for any $\mu, \nu \geq 0$, but also of type $(-\infty, \nu)$ for any $\nu \geq 0$.

$n(z)$ and denominator $d(z)$ are each of type $(m-1, m)$, so it is obvious from (2.1) that r is of type $(2m-1, 2m-1)$; it is the cancellation of the factors $1/\ell(z)$ top and bottom that makes it actually of type $(m-1, m-1)$. This is the paradox of the barycentric formula: it is of a smaller type than it looks, and its poles can be anywhere except where they appear to be. The paradox goes further in that, given any set of support points $\{z_j\}$, there is a special choice of the weights $\{w_j\}$ for which r becomes a polynomial of degree $m-1$. This is important in numerical computation, providing a numerically stable method for polynomial interpolation even in thousands of points; see [13, 16, 38] for discussion and references. However, it is not our subject here. Here we are concerned with the cases where (2.1) is truly a rational function, a situation exploited perhaps first by Salzer and then by Schneider and Werner [32, 33] and most importantly in subsequent years by Berrut and his collaborators [10, 11, 12, 25].

A key aspect of (2.1) is its interpolatory property. At each point z_j with $w_j \neq 0$, the formula is undefined, taking the form ∞/∞ (assuming $f_j \neq 0$). However, this is a removable singularity, for $\lim_{z \rightarrow z_j} r(z)$ exists and is equal to f_j . Thus if the weights w_j are nonzero, (2.1) provides a type $(m-1, m-1)$ *rational interpolant* to the data f_1, \dots, f_m at z_1, \dots, z_m . Note that such a function has $2m-1$ degrees of freedom, so roughly half of these are fixed by the interpolation conditions and the other half are not.

We summarize the properties of barycentric representations developed in the discussion above by the following theorem.

THEOREM 2.1 (Rational barycentric representations). *Let z_1, \dots, z_m be an arbitrary set of distinct complex numbers. As f_1, \dots, f_m and w_1, \dots, w_m range over all complex values, the functions described by the formula*

$$(2.5) \quad r(z) = \frac{n(z)}{d(z)} = \sum_{j=1}^m \frac{w_j f_j}{z - z_j} \bigg/ \sum_{j=1}^m \frac{w_j}{z - z_j}$$

range over the set of all rational functions of type $(m-1, m-1)$. If $w_j \neq 0$ for some j , then $r(z_j) = f_j$.

If the support points $\{z_j\}$ have no influence on the set of functions described by (2.5), one may wonder, what is the use of barycentric representations? The answer is all about numerical quality of the representation. The barycentric formula is composed from quotients $1/(z - z_j)$, and for good choices of $\{z_j\}$, these functions are independent enough to make the representation well-conditioned — often far better conditioned, in particular, than one would find with a representation $p(z)/q(z)$. The use of localized and sometimes singular basis functions is an established theme in other areas of scientific computing. *Radial basis functions*, for example, have excellent conditioning properties when they are composed of pieces that are well separated [18]. Similarly the *method of fundamental solutions*, which has had great success in solving elliptic PDEs such as Helmholtz problems, represents its functions as linear combinations of Hankel or other functions each localized at a singular point [7]. An aim of the present paper is to bring this kind of thinking to the subject of function theory. Yet another related technique in scientific computing is *discretizations of the Cauchy integral formula*, for example by the trapezoidal rule on the unit circle, to evaluate analytic functions inside a curve. The basis functions implicit in such a discretization are singular, introducing poles and hence errors of size ∞ at precisely the data points where one might expect the errors to be 0, but still the approximation may be excellent away from the curve [5, 26].

3. Core AAA algorithm. We begin with a finite *sample set* $Z \subseteq \mathbf{C}$ of $M \gg 1$ points. We assume a function $f(z)$ is given that is defined at least for $z \in Z$. This function may have an analytic expression, or it may be just a set of data values.

The AAA algorithm takes the form of an iteration for $m = 1, 2, 3, \dots$, with r represented at each step in the barycentric form (2.5). At step m we first pick the next support point z_m , and then we compute corresponding weights w_1, \dots, w_m by solving a linear least-squares problem over the subset of sample points that have not been selected as support points,

$$(3.1) \quad Z^{(m)} = Z \setminus \{z_1, \dots, z_m\}.$$

Thus at step m , we compute a rational function r of type $(m-1, m-1)$, which generically will interpolate $f_1 = f(z_1), \dots, f_m = f(z_m)$ at z_1, \dots, z_m (though not always, since one or more weights may turn out to be zero).

The least-squares aspect of the algorithm is as follows. Our aim is an approximation

$$(3.2) \quad f(z) \approx \frac{n(z)}{d(z)}, \quad z \in Z,$$

which in linearized form becomes

$$(3.3) \quad f(z)d(z) \approx n(z), \quad z \in Z^{(m)}.$$

Note that in going from (3.2) to (3.3) we have replaced Z by $Z^{(m)}$, because $n(z)$ and $d(z)$ will generically have poles at z_1, \dots, z_m , so (3.3) would not make sense over all $z \in Z$. The weights w_1, \dots, w_m are chosen to solve the least-squares problem

$$(3.4) \quad \text{minimize } \|fd - n\|_{Z^{(m)}}, \quad \|w\|_m = 1,$$

where $\|\cdot\|_{Z^{(m)}}$ is the discrete 2-norm over $Z^{(m)}$ and $\|\cdot\|_m$ is the discrete 2-norm on m -vectors. To ensure that this problem makes sense, we assume that $Z^{(m)}$ has at least m points, i.e., $m \leq M/2$.

The greedy aspect of the iteration is as follows. At step m , the next support point z_m is chosen as a point $z \in Z^{(m-1)}$ where the nonlinear residual $f(z) - n(z)/d(z)$ at step $m-1$ takes its maximum absolute value.

Assuming the iteration is successful, it terminates when the nonlinear residual is sufficiently small; we have found it effective to use a tolerance of 10^{-13} relative to the maximum of $|f(Z)|$. The resulting approximation typically has few or no numerical Froissart doublets, and if there are any, they can generally be removed by one further least-squares step to be described in Section 5. (If the convergence tolerance is too tight, the approximation will stagnate and many Froissart doublets will appear.) In the core AAA algorithm it is an approximation of type $(m-1, m-1)$.

It remains to spell out the linear algebra involved in (3.4). Let us regard $Z^{(m)}$ and $F^{(m)} = f(Z^{(m)})$ as column vectors,

$$Z^{(m)} = (Z_1^{(m)}, \dots, Z_{M-m}^{(m)})^T, \quad F^{(m)} = (F_1^{(m)}, \dots, F_{M-m}^{(m)})^T.$$

We seek a normalized column vector

$$w = (w_1, \dots, w_m)^T, \quad \|w\|_m = 1$$

that minimizes the 2-norm of the $(M - m)$ -vector

$$\sum_{j=1}^m \frac{w_j F_i^{(m)}}{Z_i^{(m)} - z_j} - \sum_{j=1}^m \frac{w_j f_j}{Z_i^{(m)} - z_j},$$

that is,

$$\sum_{j=1}^m \frac{w_j (F_i^{(m)} - f_j)}{Z_i^{(m)} - z_j}.$$

This is a matrix problem of the form

$$(3.5) \quad \text{minimize } \|A^{(m)}w\|, \quad \|w\| = 1,$$

where $A^{(m)}$ is the $(M - m) \times m$ *Löwner matrix* [1]

$$(3.6) \quad A^{(m)} = \begin{pmatrix} \frac{F_1^{(m)} - f_1}{Z_1^{(m)} - z_1} & \cdots & \frac{F_1^{(m)} - f_m}{Z_1^{(m)} - z_m} \\ \vdots & \ddots & \vdots \\ \frac{F_{M-m}^{(m)} - f_1}{Z_{M-m}^{(m)} - z_1} & \cdots & \frac{F_{M-m}^{(m)} - f_m}{Z_{M-m}^{(m)} - z_m} \end{pmatrix}.$$

We will solve (3.5) using the singular value decomposition (SVD), taking w as the final right singular vector in a reduced SVD $A = U\Sigma V^*$. Along the way it is convenient to make use of the $(M - m) \times m$ *Cauchy matrix*

$$(3.7) \quad C = \begin{pmatrix} \frac{1}{Z_1^{(m)} - z_1} & \cdots & \frac{1}{Z_1^{(m)} - z_m} \\ \vdots & \ddots & \vdots \\ \frac{1}{Z_{M-m}^{(m)} - z_1} & \cdots & \frac{1}{Z_{M-m}^{(m)} - z_m} \end{pmatrix},$$

whose columns define the basis in which we approximate. If we define diagonal left and right scaling matrices by

$$(3.8) \quad S_F = \text{diag}(F_1^{(m)}, \dots, F_{M-m}^{(m)}), \quad S_f = \text{diag}(f_1, \dots, f_m),$$

then we can construct $A^{(m)}$ from C using the identity

$$(3.9) \quad A^{(m)} = S_F C - C S_f,$$

and once w is found with the SVD, we can compute $(M - m)$ -vectors N and D with

$$(3.10) \quad N = C(wf), \quad D = Cw.$$

These correspond to the values of $n(z)$ and $d(z)$ at points $z \in Z^{(m)}$. (Since M will generally be large, it is important that the sparsity of S_F is exploited in the multiplication of (3.9).) Finally, to get an M -vector R corresponding to $r(z)$ for all $z \in Z$, we set $R = F$ and then $R(Z^{(m)}) = N/D$.

After the AAA algorithm terminates (assuming $w_j \neq 0$ for all j), one has a rational approximation $r(z) = n(z)/d(z)$ in barycentric form. The zeros of d , which are (generically) the poles of r , can be computed by solving an $(m+1) \times (m+1)$ generalized eigenvalue problem in arrowhead form [25, Sec. 2.3.3],

$$(3.11) \quad \begin{pmatrix} 0 & w_1 & w_2 & \cdots & w_m \\ 1 & z_1 & & & \\ & & z_2 & & \\ & & & \ddots & \\ & & & & z_m \\ 1 & & & & \end{pmatrix} = \lambda \begin{pmatrix} 0 & & & & \\ & 1 & & & \\ & & 1 & & \\ & & & \ddots & \\ & & & & 1 \end{pmatrix}.$$

At least two of the eigenvalues of this problem are infinite, and the remaining $m-1$ are the zeros of d . A similar computation with w_j replaced by $w_j f_j$ gives the zeros of $n(z)$.

The following proposition collects some elementary properties of the core AAA algorithm. We say “a” instead of “the” in view of the fact that in cases of ties in the greedy choice at each step, AAA approximants are not unique.

PROPOSITION 3.1. *Let $r(z)$ be a AAA approximant at step m of a function $f(z)$ on a set Z (computed in exact arithmetic). The following statements refer to AAA approximants at step m , and a and b are complex constants.*

Affineness in f . For any $a \neq 0$ and b , $ar(z) + b$ is an approximant of $af(z) + b$ on Z .

Affineness in z . For any $a \neq 0$ and b , $r(az + b)$ is an approximant of $f(az + b)$ on $(Z - b)/a$.

Monotonicity. The linearized residual norm $\sigma_{\min}(A^{(m)}) = \|fd - n\|_{Z^{(m)}}$ is a nonincreasing function of m .

Proof. These properties are straightforward and we do not spell out the arguments except to note that the monotonicity property follows from the fact that $A^{(m)}$ is obtained from $A^{(m-1)}$ by deleting one row and appending one column. Since the minimum singular vector for $A^{(m-1)}$ (padded with one more zero) is also a candidate singular vector of $A^{(m)}$, we must have $\sigma_{\min}(A^{(m)}) \leq \sigma_{\min}(A^{(m-1)})$. \square

One might ask, must the monotonicity be strict, with $\sigma_{\min}(A^{(m)}) < \sigma_{\min}(A^{(m-1)})$ if $\sigma_{\min}(A^{(m-1)}) \neq 0$? So far as we are aware, the answer is no. An equality $\sigma_{\min}(A^{(m)}) = \sigma_{\min}(A^{(m-1)})$ implies $f(z_m)d_{m-1}(z_m) = n_{m-1}(z_m)$, where z_m is the support point selected at step m . This in turn implies $d_{m-1}(z_m) = n_{m-1}(z_m) = 0$, since otherwise we could divide by $d_{m-1}(z_m)$ to find $f(z_m) - n_{m-1}(z_m)/d_{m-1}(z_m) = 0$, which would contradict the greedy choice of z_m . But so far as we know, the possibility $d_{m-1}(z_m) = n_{m-1}(z_m) = 0$ is not excluded.

Since the AAA algorithm involves SVDs of dimensions $(M-j) \times j$ with $j = 1, 2, \dots, m$, its complexity is $O(Mm^3)$ flops. This is usually modest since in most applications m is small.

4. Matlab code. The Matlab code `aaa.m`, shown in Figure 4.1 and available in Chebfun [16], is intended to be readable as well as computationally useful and makes the AAA algorithm fully precise. The code closely follows the algorithm description above, differing in just one detail for programming convenience: instead of working

```

function [r,pol,res,zer,z,f,w,errvec] = aaa(Z,F,tol,mmax)
% aaa rational approximation of data F on set Z
% [r,pol,res,zer,z,f,w,errvec] = aaa(Z,F,tol,mmax)
%
% Input: Z = vector of sample points
% F = vector of data values, or a function handle
% tol = relative tolerance tol, set to 1e-13 if omitted
% mmax: max type is (mmax-1,mmax-1), set to 100 if omitted
%
% Output: r = AAA approximant to F (function handle)
% pol,res,zer = vectors of poles, residues, zeros
% z,f,w = vectors of support pts, function values, weights
% errvec = vector of errors at each step

M = length(Z); % number of sample points
if nargin<3, tol = 1e-13; end % default relative tol 1e-13
if nargin<4, mmax = 100; end % default max type (99,99)
if ~isfloat(F), F = F(Z); end % convert function handle to vector
Z = Z(:); F = F(:); % work with column vectors
SF = spdiags(F,0,M,M); % left scaling matrix
J = 1:M; z = []; f = []; C = []; % initializations
errvec = []; R = mean(F);
for m = 1:mmax % main loop
    [~,j] = max(abs(F-R)); % select next support point
    z = [z; Z(j)]; f = [f; F(j)]; % update support points, data values
    J(J==j) = []; % update index vector
    C = [C 1./(Z-Z(j))]; % next column of Cauchy matrix
    Sf = diag(f); % right scaling matrix
    A = SF*C - C*Sf; % Loewner matrix
    [~,~,V] = svd(A(J,:),0); % SVD
    w = V(:,m); % weight vector = min sing vector
    N = C*(w.*f); D = C*w; % numerator and denominator
    R = F; R(J) = N(J)./D(J); % rational approximation
    err = norm(F-R,inf); % max error at sample points
    errvec = [errvec; err]; % stop if converged
    if err <= tol*norm(F,inf), break, end
end
r = @(zz) feval(@rhandle,zz,z,f,w); % AAA approximant as function handle
[pol,res,zer] = prz(r,z,f,w); % poles, residues, and zeros
[r,pol,res,zer,z,f,w] = ...
    cleanup(r,pol,res,zer,z,f,w,Z,F); % remove Frois. doublets (optional)

function [pol,res,zer] = prz(r,z,f,w) % compute poles, residues, zeros
m = length(w); B = eye(m+1); B(1,1) = 0;
E = [0 w.'; ones(m,1) diag(z)];
pol = eig(E,B); pol = pol(~isinf(pol)); % poles
dz = 1e-5*exp(2i*pi*(1:4)/4);
res = r(bsxfun(@plus,pol,dz))*dz.'/4; % residues
E = [0 (w.*f).'; ones(m,1) diag(z)];
zer = eig(E,B); zer = zer(~isinf(zer)); % zeros

function r = rhandle(zz,z,f,w) % evaluate r at zz
zv = zz(:); % vectorize zz if necessary
CC = 1./bsxfun(@minus,zv,z. '); % Cauchy matrix
r = (CC*(w.*f))./(CC*w); % AAA approx as vector
ii = find(isnan(r)); % find values NaN = Inf/Inf if any
for j = 1:length(ii)
    r(ii(j)) = f(find(zv(ii(j))==z)); % force interpolation there
end
r = reshape(r,size(zz)); % AAA approx

```

FIG. 4.1. Matlab code for the AAA algorithm, returning r as a function handle. The optional code `cleanup` is listed in Section 5. Commenting out this line gives the “core” AAA algorithm.

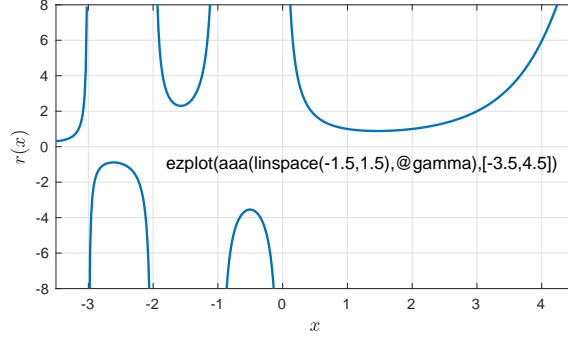


FIG. 4.2. AAA approximation to $f(x) = \Gamma(x)$ produced by the command shown. This is a rational approximant of type (9,9) whose first four poles match 0, -1 , -2 , and -3 to 15, 15, 7, and 3 digits, respectively, with corresponding residues matching 1, -1 , $1/2$, and $-1/6$ to similar accuracy.

with a subset $Z^{(m)}$ of size $M - m$ of Z , we use an index vector J that is a subset of size $M - m$ of $1:M$. The matrices C and A always have M rows, and the SVD is applied not to all of A but to the submatrix with rows indexed by J .

We have modeled `aaa` on the code `ratdisk` of [22], and in particular, the object `r` that it returns is a function handle that can evaluate r at a scalar, vector, or matrix of real or complex numbers. The code is flexible enough to cover a wide range of computations, and was used for all the applications of Section 6. The code as listed does not include the safeguards one would expect in a fully developed piece of software, but its Chebfun realization (version 5.6.0, December 2016) does have some of these features.

Computing a AAA approximation with `aaa` can be as simple as calling `r = aaa(Z,f)` and then evaluating `r(z)`, where z is a scalar or vector or matrix of real or complex numbers. For example, Figure 4.2 shows a good approximation of the gamma function on $[-3.5, 4.5]$ extrapolated from 100 samples in $[-1.5, 1.5]$, all invoked by the line of Matlab displayed in the figure.

For a second illustration, shown in Figure 4.3, we call `aaa` with the sequence

```
Z = exp(linspace(-.5,.5+.15i*pi,1000));
F = @(z) tan(pi*z/2);
[r,pol,res,zer] = aaa(Z,F);
```

The set Z is a spiral of 1000 points winding $7\frac{1}{2}$ times around the origin in the complex plane. When the code is executed, it takes $m = 12$ steps to convergence with the following errors:

```
2.49e+01, 4.28e+01, 1.71e+01, 8.65e-02, 1.27e-02, 9.91e-04,
5.87e-05, 1.29e-06, 3.57e-08, 6.37e-10, 1.67e-11, 1.30e-13
```

The first pair of poles of r match the poles of f at ± 1 to 15 digits, the next pair match ± 3 to 7 digits, and the third pair match ± 5 to 3 digits. The zeros of r show a similar agreement with those of f .

Poles

Zeros

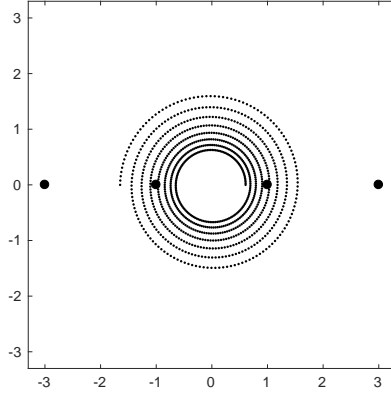


FIG. 4.3. Approximation of $f(z) = \tan(\pi z/2)$ on a set of 1000 points lying along a spiral in the complex plane. The inner pair of computed poles (dots) match the corresponding poles of f to 15 digits, and the second pair match to 7 digits.

1.0000000000000000 + 9.01e-17i	-0.0000000000000000 - 2.14e-15i
-1.0000000000000000 + 5.55e-19i	2.0000000000000839 - 4.77e-12i
3.000000100 - 4.09e-08i	-2.000000000000043 - 4.38e-12i
-3.000000065 - 5.83e-08i	4.0000427 - 1.25e-05i
5.002693 - 5.61e-04i	-4.0000355 - 1.73e-05i
-5.002439 - 7.47e-04i	6.0461 - 6.74e-03i
7.3273 - 3.46e-02i	-6.0435 - 8.67e-03i
-7.3154 - 4.29e-02i	9.387 - 1.17e-01i
13.65 - 3.74e-01i	-9.350 - 1.39e-01i
-13.54 - 3.74e-01i	-26.32 - 1.85e+00i
-47.3 - 3.60e+02i	26.81 - 1.80e+00i

5. Removing numerical Froissart doublets. In many applications, the AAA algorithm finishes with a clean rational approximation r , with no numerical Froissart doublets. Sometimes, however, these artifacts appear, and one can always generate them by setting the convergence tolerance to 0 and taking the maximal step number `mmax` to be sufficiently large. Our method of addressing this problem, implemented in the code `cleanup` listed in Figure 5.1, is as follows. We identify spurious poles by their residues $< 10^{-13}$, remove the nearest support points from the set of support points, and then solve the least-squares problem (3.4) by a new SVD calculation.

For an example from [22], suppose the function $f(z) = \log(2 + z^4)/(1 - 16z^4)$ is approximated in 1000 roots of unity with tolerance 0. The left image of Figure 5.2 shows what happens if this is done with `cleanup` disabled: the code runs to $m = 100$, at which point there are 58 numerical Froissart doublets near the unit circle, marked in red. The right image, with `cleanup` enabled, shows just one Froissart doublet, an artifact that appeared when the first 58 were eliminated. The other poles comprise four inside the unit circle, matching poles of f , and collections of poles lining up along branch cuts of f ; see Application 6.2.

6. Applications. In this section we present eight applications computed with `aaa`. Different applications raise different mathematical and computational issues, which we discuss in some generality in each case while still focusing on the particular

```

function [r,pol,res,zer,z,f,w] = cleanup(r,pol,res,zer,z,f,w,Z,F)
m = length(z); M = length(Z);
ii = find(abs(res)<1e-13);           % find negligible residues
ni = length(ii);
if ni == 0, return, end
fprintf('%d Froissart doublets\n',ni)
for j = 1:ni
    azp = abs(z-pol(ii(j)));
    jj = find(azp == min(azp),1);
    z(jj) = []; f(jj) = [];         % remove nearest support points
end
for j = 1:length(z)
    F(Z==z(j)) = []; Z(Z==z(j)) = [];
end
m = m-length(ii);
SF = spdiags(F,0,M-m,M-m);
Sf = diag(f);
C = 1./bsxfun(@minus,Z,z. ');
A = SF*C - C*Sf;
[~,~,V] = svd(A,0); w = V(:,m);    % solve least-squares problem again
r = @(zz) feval(@rhandle,zz,z,f,w);
[pol,res,zer] = prz(r,z,f,w);       % poles, residues, and zeros

```

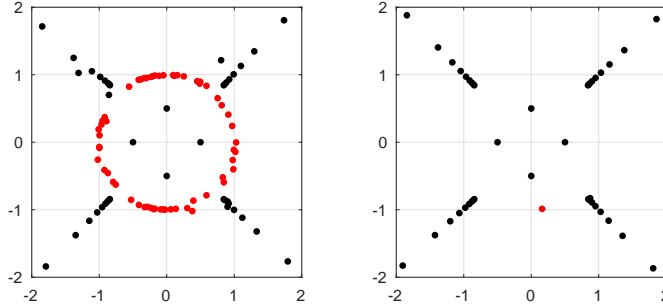
FIG. 5.1. *Matlab code for removing numerical Froissart doublets.*

FIG. 5.2. *If the AAA algorithm is run with `tol` = 0 and with the `cleanup` option disabled, as in the left image, numerical Froissart doublets appear. Here we see approximation of $f(z) = \log(2 + z^4)/(1 - 16z^4)$ in 1000 roots of unity, with red dots marking poles with residues of absolute value $< 10^{-13}$. The right image shows the result if `cleanup` is enabled. The result is much the same, but with no numerical doublets at all, if the algorithm is run with its default tolerance 10^{-13} .*

example for concreteness. Application 6.6 is the only one in which any numerical Froissart doublets were found (6 of them); they are removed by `cleanup`.

6.1. Analytic functions in the unit disk. Let Δ be the closed unit disk $\Delta = \{z \in \mathbb{C} : |z| \leq 1\}$, and suppose f is analytic on Δ . Then f can be approximated on Δ by polynomials, with exponential convergence as $n \rightarrow \infty$, and if f is not entire, then the asymptotically optimal rate of convergence is $O_\varepsilon(\rho^{-n})$, where ρ is the radius of the disk of analyticity of f about $z = 0$.³ Truncated Taylor series achieve this rate, as do interpolants in roots of unity or in any other point sets uniformly distributed on

³We use the symbol O_ε defined as follows: $g(n) = O_\varepsilon(\rho^{-n})$ if for all $\varepsilon > 0$, $g(n) = O((\rho - \varepsilon)^{-n})$ as $n \rightarrow \infty$. This enables us to focus on exponential convergence rates without being distracted by lower-order algebraic terms.

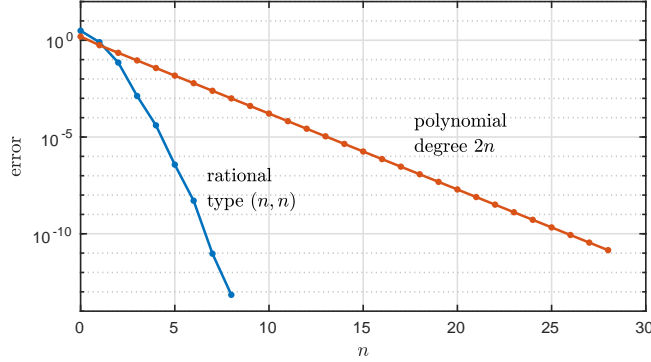


FIG. 6.1. *Application 6.1. Even for an analytic function on the unit disk, rational approximations may be more efficient than polynomials. Here $f(z) = \tan(z)$ is approximated by the AAA algorithm in 128 points on the unit circle.*

the unit circle as $n \rightarrow \infty$ [20, 41]. Algorithms for computing polynomial interpolants in roots of unity are discussed in [5]. By the maximum modulus principle, any polynomial approximation on the unit circle will have the same maximum error over the unit disk.

Rational approximations may be far more efficient, however, depending on the behavior of f outside Δ . For example, consider the function $f(z) = \tan(z)$. Because of the poles at $\pm\pi/2 \approx 1.57$, polynomial approximations can converge no faster than $O_\varepsilon(1.57^{-n})$, so that $n \geq 52$ will be required, for example, for 10-digit accuracy. Rational approximations can do much better since they can capture poles outside the disk. Figure 6.1 shows maximum-norm approximation errors for polynomial and type (ν, ν) rational AAA approximation of this function in $M = 128$ equispaced points on the unit circle. (The results would be much the same with $M = \infty$.) We see that the rational approximation of type $(7, 7)$ is more accurate than the polynomial of degree 52.

In principle, there is no guarantee that AAA rational approximations must be free of poles in the interior of Δ . In this example no such poles appear at any step of the iteration, however, so the errors would be essentially the same if measured over the whole disk. Incidentally, one may note that since f is an odd function with no poles in the disk, it is natural to approximate it by rational functions of type (μ, ν) with ν even. This is approximately what happens as the algorithm is executed, for each approximation of type $(m-1, m-1)$ with $m-1$ odd has a pole close to ∞ ; in that sense the rational function is nearly of type $(m-1, m-2)$. For $m-1 = 3$ there is a pole at 5.4×10^{14} , for $m-1 = 5$ there is a pole at 8.8×10^{11} , and so on. The remaining poles are real numbers lying in approximate plus/minus pairs about $z = 0$, with the inner pair closely approximating $\pm\pi/2$ for $m-1 = 6$ and higher. See Section 8 for further remarks about approximating even and odd functions.

This experiment confirms that rational functions may have advantages over polynomials on the unit disk, even for approximating analytic functions. A different question is, how does the AAA approximant compare with rational approximations computed by other methods such as the `ratdisk` algorithm of [22]? For this example, other algorithms can do about equally well, but the next example is different.

6.2. Analytic functions with nearby branch points; comparison with `ratdisk`. When the singularities of a function $f(z)$ outside of the disk are just poles,

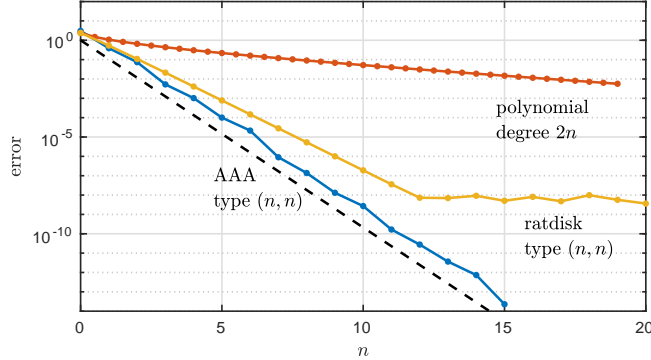


FIG. 6.2. *Application 6.2. Rational functions are also effective for approximating $f(z) = \log(1.1 - z)$ in 256 points on the unit circle. This function has a branch point outside the unit disk instead of poles. The slope of the dashed line marks the convergence rate for best type (n, n) approximations on the unit disk.*

a rational approximation on the unit circle can “peel them off” one by one, leading to supergeometric convergence as in Figure 6.1. Branch point singularities are not so simple, but as is well known, rational approximation is effective here too. For example, Figure 6.2 shows polynomial and AAA rational approximations to $f(z) = \log(1.1 - z)$ in 256 roots of unity. The degree $2n$ polynomials converge at the rate $O_\varepsilon(1.1^{-2n})$, while the rational approximations converge at a rate $O_\varepsilon(\rho^{-n})$ with $\rho \approx 9.3$. The precise constant for best rational approximations can be determined by methods of potential theory due to Gonchar, Parfenov, Prokhorov, and Stahl and summarized in the final paragraph of [28]. In fact $\rho = R^2$, where $R \approx 3.046$ is the outer radius of the annulus with inner radius 1 that is conformally equivalent to the domain exterior to the unit disk and the slit $[1.1, \infty)$. A formula for R is given on p. 609 of [23]:

$$(6.1) \quad R = \exp\left(\frac{\pi K(\sqrt{1-\kappa^2})}{4K(\kappa)}\right), \quad \kappa = (c - \sqrt{c^2 - 1})^2, \quad c = 1.1,$$

where $K(\kappa)$ is the complete elliptic integral of the first kind.

It is well known that when rational functions approximate functions with branch cuts, most of the poles tend to line up along branch cuts [4, 36]. This effect is shown in Figure 6.3. Apart from the zero near 0.1 that matches the zero there of f , the zeros and poles of r interlace along a curve close to the branch cut $[1, \infty)$. The fact that they end up slightly below rather than above the cut is of no significance except in illustrating that the core AAA algorithm does not impose a real symmetry. As it happens, for this problem the first support point is $z_1 = 1$, the second is $z_2 = -1$, and then the real symmetry is broken at step 3 with the selection of $z_3 \approx 0.87 - 0.49i$.

Figure 6.2 also includes a third curve showing convergence for a technique based on representation of a rational function by a quotient of polynomials $p(z)/q(z)$ — the **ratdisk** approximant of [22], computed by linearized least-squares minimization of $\|fq - p\|$ in 256 roots of unity. (In Chebfun we calculate such an approximant with the command `[p,q,r] = ratinterp(@(z) log(1.1-z),n,n,256,'unitroots')`.) This linearized problem uses bases $1, z, z^2, \dots$ in the numerator and the denominator, whereas AAA uses partial fraction bases, and that is why the rational approximants need not match even for small n , when rounding error is not an issue. For larger n ,

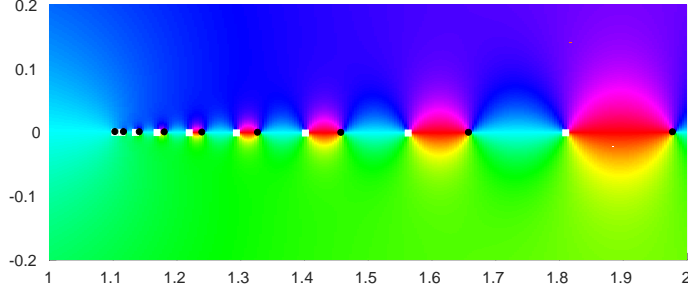


FIG. 6.3. Application 6.2, continued. A phase portrait [42] of the rational approximant r shows zeros (black dots) and poles (white squares) interlacing along the branch cut $[1, \infty)$.

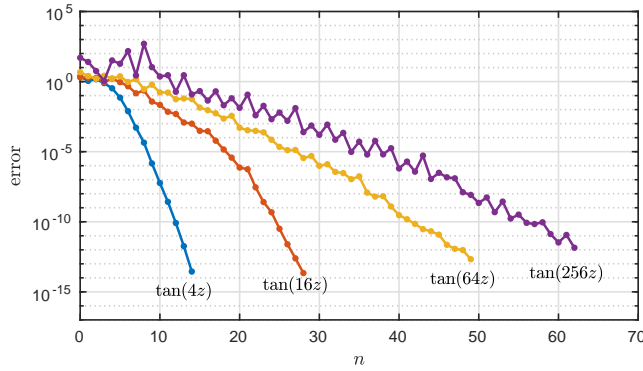


FIG. 6.4. Application 6.3. Errors in type (n, n) AAA approximation of $\tan(\beta z)$ with $\beta = 4, 16, 64, 256$ in 1000 points on the unit circle.

`ratdisk` additionally encounters numerical instability because its numerator p and denominator q both become very small for values of z near the branch cut, leading to cancellation error.

6.3. Meromorphic functions in the unit disk I. Now suppose f is analytic on the unit circle and meromorphic in Δ , which means, it is analytic in Δ apart from poles, which will necessarily be finite in number. If p is the number of poles counted with multiplicity, then f can be approximated on the unit circle by rational functions of type (μ, ν) as $\mu \rightarrow \infty$ for any $\nu \geq p$. For $\nu < p$ this is not possible in the sense of approximation to arbitrary accuracy, but that is not the whole story, because one may be interested in a fixed accuracy such as 8 or 16 digits. Suppose for example that $f(z)$ is nonzero for $|z| = 1$ with winding number $-q$ there for some $q > 0$, which implies that the number of poles in the unit disk exceeds the number of zeros by q . Then no type (μ, ν) rational function r with $\nu < q$ can differ from f on $|z| = 1$ by less than $\min_{|z|=1} |f(z)|$, because such an r would have to have winding number $-q$ too (this is Rouché's theorem). On the other hand for $\nu \geq q$, a rational approximation can get the winding number right and good accuracy may be possible.

For example, Figure 6.4 shows errors in AAA approximation of $\tan(\beta z)$ with

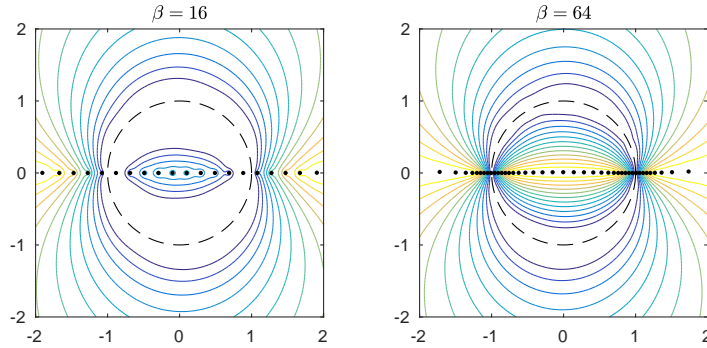


FIG. 6.5. Application 6.3 continued, showing more information about the final approximations r of Figure 6.4 in the cases $\beta = 16$ and 64 . Contours of the error $|f(z) - r(z)|$ mark powers of 10 from yellow (10^{-1}) to dark blue (10^{-12}). With $\beta = 16$, all the poles of f are approximated by poles of r and $r \approx f$ throughout Δ . With $\beta = 64$, f has more poles than r , and r approximates f on the circle but not throughout Δ .

$\beta = 4, 16, 64, 256$ in 1000 equispaced points on the unit circle. Robust superlinear convergence is observed in all cases. Now these four functions have 2, 10, 40, and 162 poles in the unit disk, respectively, and from the figure we see that they are approximated on the unit circle to 13-digit accuracy by rational functions of types (14, 14), (28, 28), (49, 49) and (62, 62). Clearly the fourth approximation, at least, cannot be accurate throughout the unit disk, since it does not have enough poles. The right image of Figure 6.5 confirms that it is accurate near the unit circle, but not throughout the disk. By contrast the left image of the figure, for the simpler function f with $\beta = 16$, shows good accuracy throughout the disk. This example highlights fundamental facts of rational approximation: one cannot assume without careful reasoning that an approximation accurate on one set must be accurate elsewhere, even in a region enclosed by a curve, nor that it provides information about zeros or poles of the function being approximated away from the set of approximation. An approximation on a closed curve does however tell you the winding number, hence the *difference* between numbers of poles and zeros of the underlying function in the region enclosed.

We have spoken of the possibility of accuracy “throughout Δ .” There is a problem with such an expression, for even if the poles of r in the unit disk match those of f closely, they will not do so exactly. Thus, mathematically speaking, the maximal error in the disk will almost certainly be ∞ for all rational approximations of functions that have poles. Nevertheless one feels that it ought be possible to say, for example, that $1/(z - 10^{-15})$ is a good approximation to $1/z$. One way to do this is to measure the difference between complex numbers w_1 and w_2 not by $|w_1 - w_2|$ but by the chordal metric on the Riemann sphere. This and other possibilities are discussed in [8].

6.4. Meromorphic functions in the unit disk II. If the aim is approximation throughout the unit disk, the simplest approach is to distribute sample points inside the disk as well as on the circle, assuming function values are known there. Figures 6.6 and 6.7 repeat Figures 6.4 and 6.5, but now with 3000 points randomly distributed in the unit disk in addition to 1000 points on the unit circle. Note that n must now be larger for convergence with $\beta = 64$ and especially 256. (This last case leads to large matrices and the only slow computation of this article, about 30 seconds

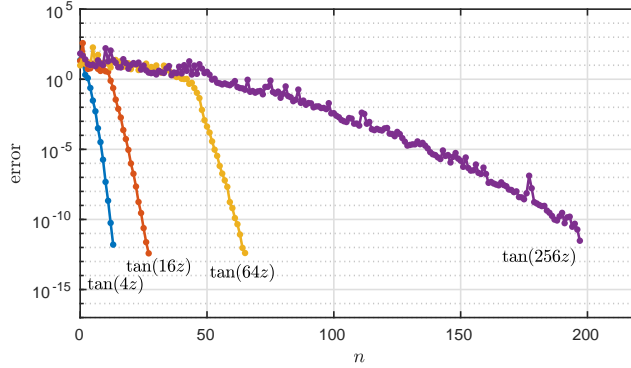


FIG. 6.6. Application 6.4. Repetition of Figure 6.4 for a computation with 3000 points in the interior of the unit disk as well as 1000 points on the boundary. Higher values of n are now needed to achieve 13-digit accuracy, but all the poles are captured. If many more than 3000 points were used, the final curve would not show any convergence until $n \geq 162$.

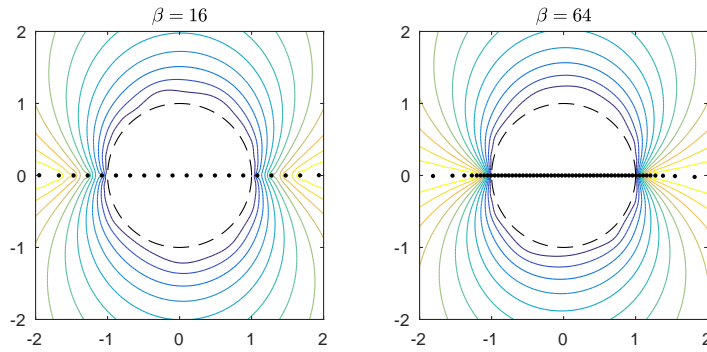


FIG. 6.7. Application 6.4, continued, a repetition of Figure 6.5 for the computation with points in the interior of the disk. Now the rational approximants are accurate throughout Δ .

on our laptops.) We mentioned above that f has 2, 10, 40, and 162 poles in Δ for the four values of β . The AAA approximants match the first three of these numbers, but the fourth approximation comes out with 164 poles in Δ , the two extra ones being complex numbers near the real axis, Froissart doublets of the non-numerical variety, with residues on the order of 10^{-7} and 10^{-11} . If the number of points in the disk is doubled to 6000, they go away.

6.5. Approximation in other connected domains. The flexibility of AAA approximation becomes most apparent for approximation on a non-circular domain Z . Here the observations of the last few pages about the advantages of barycentric representations compared with quotients of polynomials $p(z)/q(z)$ still apply. In addition, the latter representations have the further difficulty on a non-circular domain Z that it is necessary to work with a good basis for polynomials on Z to avoid exponential ill-conditioning. If E is connected, the well-known choice is the basis of Faber polynomials, which might be calculated a priori or approximated on the fly in various ways [20]. The AAA algorithm circumvents this issue by using a partial fraction

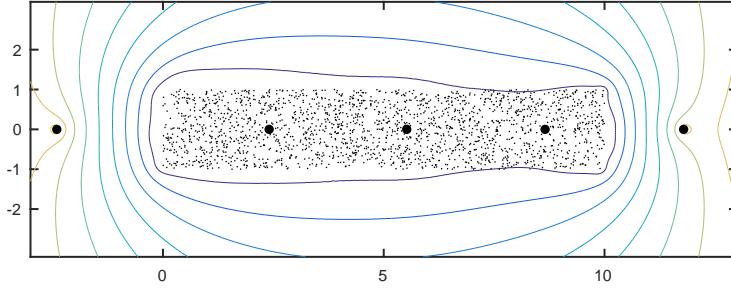


FIG. 6.8. Application 6.5. Approximation of $1/J_0(z)$ in 2000 random points in a rectangle in the complex plane. Contours mark levels $10^{-12}, \dots, 10^{-1}$ of the error $|f(z) - r(z)|$, as in Figures 6.5 and 6.7, and the dots are the poles of the rational approximant.

basis constructed as the iteration proceeds. For example, Figure 6.8 shows contours of the AAA approximant of the reciprocal Bessel function $1/J_0(z)$ in 2000 uniformly distributed random points in the rectangle defined by the corners $\pm i$ and $10 \pm i$. The algorithm exits at step $m = 13$ with an approximation of type $(12, 12)$. The computed poles in the domain rectangle are almost exactly real, even though no real symmetry has been imposed, and almost exactly equal to the poles of f in this region.

Poles of f in rectangle	Poles of r in rectangle
2.404825557695780	2.404825557695776 - 0.000000000000001i
5.520078110286327	5.520078110286310 - 0.000000000000000i
8.653727912911013	8.653727912911007 + 0.000000000000002i

6.6. Approximation in disconnected domains. One of the striking features of rational functions is their ability to approximate efficiently on disconnected domains and discretizations thereof. (This is related to the power of IIR as opposed to FIR filters in digital signal processing [30].) As an example, Figure 6.9 shows approximation contours for approximation of $f(z) = \text{sign}(\text{Re}(z))$ on a set Z consisting of 1000 points equally spaced around a square in the left half-plane (center -1.5 , side length 2) and 1000 points equally spaced on a circle in the right half-plane (center 1.5 , diameter 2). This is the only one of our applications in which numerical Froissart doublets appear. Convergence is achieved at $m = 51$, and then six doublets are removed by `cleanup`. One would expect the resulting approximant to be of type $(44, 44)$, but in fact the type is $(43, 43)$ because one weight w_j is identically zero as a consequence of the Löwner matrix having half its entries exactly zero.

There is not much literature on methods for practical rational approximation on disconnected domains. If one uses a representation of r as a quotient of polynomials $r(z) = p(z)/q(z)$, the problem of finding well-conditioned bases for p and q arises again. The generalizations of Faber polynomials for disconnected domains are known as *Faber–Walsh polynomials*, but they seem to have been little used except in [34].

6.7. Approximation of $|x|$ on $[-1, 1]$. Our next application concerns the first of the “two famous problems” discussed in Chapter 25 of [38]: the rational approximation of $f(x) = |x|$ on $[-1, 1]$. In the 1910s it was shown by Bernstein and others that polynomial approximants of this function achieve at best $O(n^{-1})$ accuracy, whereas a celebrated paper of Donald Newman in 1964 proved that rational approximations can have root-exponential accuracy [29]; the precise optimal convergence rate was

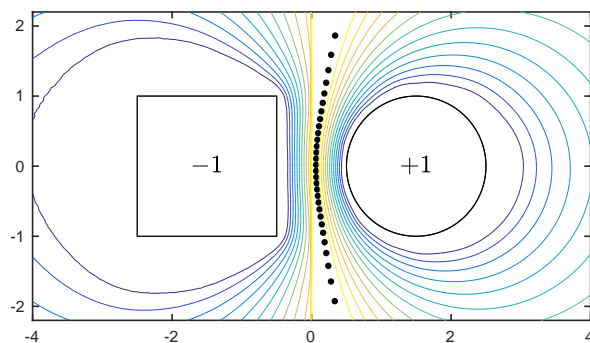


FIG. 6.9. Application 6.6. Approximation of $\text{sign}(\text{Re}(z))$ in 2000 points on a disconnected set consisting of a square and a circle in the complex plane, with contour levels as before. Six numerical Froissart doublets have been automatically removed.

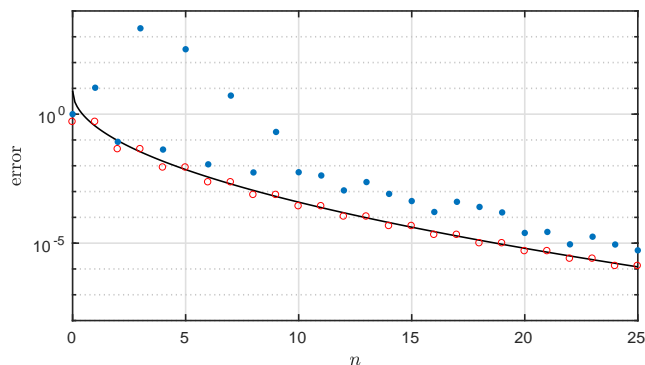


FIG. 6.10. Application 6.7. Upper dots: errors in AAA approximation of $|x|$ in 200,000 points in $[-1, 1]$. Odd values of $n \geq 3$ give approximations with poles in $[-1, 1]$, while the even- n approximations are pole-free for $n \leq 6$. Because of the large value of M , this computation took about 8 seconds in Matlab on a desktop machine. Lower dots: best approximation errors for the same problem, superimposed on the asymptotic result of [35].

eventually shown to be $E_{nn}(|x|) \sim 8 \exp(-\pi\sqrt{n})$ [35].

Computing good rational approximations of $|x|$ is notoriously difficult. Chebfun's Remez algorithm code for computing best approximations, for example, fails at degree about $(10, 10)$, though outstanding high-precision results were obtained by Varga and Carpenter in 1985 [40]. The difficulty is that good approximations need poles exponentially clustered in conjugate pairs along the imaginary axis near $x = 0$, with the extrema of the equioscillating error curve similarly clustered on the real axis.

Suppose we apply the AAA algorithm with a set Z of 200,000 equispaced points in $[-1, 1]$. The results in Figure 6.10 show interesting behavior. Steps $n = 0, 1, 2$ are normal, with the error at $n = 2$ not far from optimal. The approximations with $n = 3, 5, 7, \dots$, however, have large errors on the sample set Z and in fact infinite errors on $[-1, 1]$. In these cases the AAA algorithm must use an odd number of poles in approximating an even function, so at least one of them must be real, and it falls in $[-1, 1]$. These Froissart doublets are not numerical: they would appear even in exact

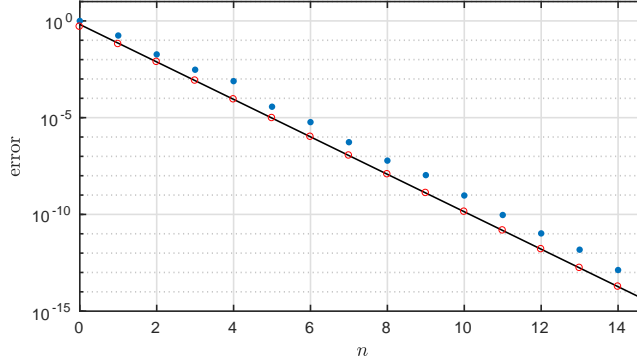


FIG. 6.11. Application 6.8. Upper dots: errors in AAA approximation of $\exp(x)$ in 2000 points in $(-\infty, 0]$ logarithmically spaced from -10^4 to -10^{-3} . This computation took about 1 second in Matlab on a desktop machine. Lower dots: best approximation errors for the same problem, superimposed on the asymptotic result of [3].

arithmetic. Eventually the dots cease to fall on two clear curves distinguishing even and odd n , and in fact, the approximations from $n = 8$ on all have at least one pole in $[-1, 1]$, though this is not always apparent in the data of the figure.

To approximate $|x|$ on $[-1, 1]$, one can do much better by exploiting symmetry and approximating \sqrt{x} on $[0, 1]$, an equivalent problem (see p. 213 of [38]). This transformation enables successful approximations up to $n = 80$, better than 10 digits of accuracy, with no poles in the interval of approximation. This is highly satisfactory as regards the $|x|$ problem, but it is not a strategy one could apply in all cases. The fact is that the core AAA algorithm risks introducing unwanted poles when applied to problems involving real functions on real intervals, and the reason is not one of even or odd symmetry.

6.8. Approximation of $\exp(x)$ on $(-\infty, 0]$. Our final core AAA application is the second of the “two famous problems” of [38]: the rational approximation of $f(x) = \exp(x)$ on $(-\infty, 0]$. As told in [38], many researchers have contributed to this problem over the years, including Cody, Meinardus and Varga, Trefethen and Gutknecht, Magnus, Gonchar and Rakhmanov, and Aptekarev. The sharp result is that minimax approximation errors for type (ν, ν) approximation decrease geometrically as $\nu \rightarrow \infty$ at a rate $\sim 2H^{n+1/2}$, where H , known as *Halphen’s constant*, is approximately $1/9.28903$ [3]. The simplest effective way to compute these approximants accurately is to transplant $(-\infty, 0]$ to $[-1, 1]$ by a Möbius transformation and then apply CF approximation [39]. Figure 6.11 shows that one can come within a factor of 10 of optimality by applying the AAA algorithm with Z as the set of 4000 points logarithmically spaced from -10^4 to -10^{-3} . (We loosened the tolerance from 10^{-13} to 10^{-12} .) Note that in this case the AAA algorithm is working with little trouble on a set of points ranging in amplitude by seven orders of magnitude.

7. Modified algorithm to treat large and small data symmetrically. On the Riemann sphere, the point $z = \infty$ has no special status, and a function meromorphic on the whole sphere must be rational. From this point of view every rational function has equal numbers of poles and zeros: if there are μ finite zeros and ν finite poles, then $z = \infty$ will be a pole of order $\mu - \nu$ if $\mu > \nu$ and a zero of order

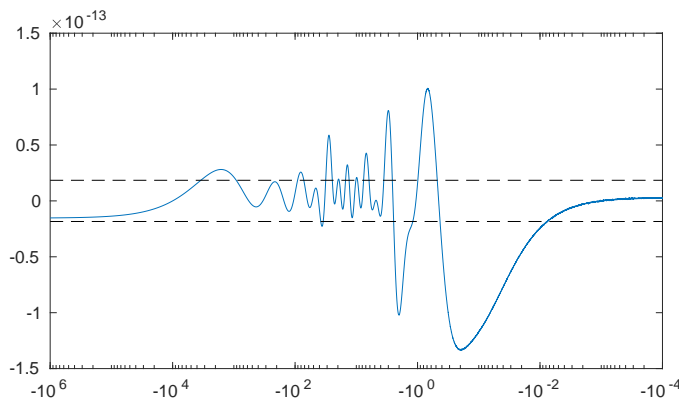


FIG. 6.12. Application 6.8, continued. Error curve $f(x) - r(x)$, $x \in (-\infty, 0]$, for the final approximant, of type $(14, 14)$, which not-quite-equioscillates between 26 local extrema of alternating signs. This approximation is of type $(14, 14)$, so the error curve for the minimax rational function would have 30 equioscillatory extreme points, with the amplitude shown by the dashed lines.

$\nu - \mu$ if $\nu > \mu$. Moreover, if r is a rational function with ν poles and ν zeros on the sphere, then the same is true of $1/r$.

One may ask whether the AAA algorithm respects such symmetries. If r is a AAA approximant of f of type $(m-1, m-1)$ on a given set Z , will $1/r$ be the corresponding approximant of $1/f$? Will $r(1/z)$ be the approximant of $f(1/z)$ on $1/Z$? The answer is yes to the second question but no to the first for the AAA algorithm as we have formulated it, but a small change in the algorithm will ensure this property. In the linear least-squares problem (3.4) solved at each step, the quantity associated with the point z is $|f(z)d(z) - n(z)|$. To achieve symmetry it is enough to change this to $|d(z) - n(z)/f(z)|$ at each point z where $|f(z)| > 1$. For points with $f(z) \neq \infty$ this amounts to dividing the row of the matrix A of (3.9) corresponding to z by $f(z)$. (The same scaling was introduced in [24] for reasons of numerical stability.) On the Riemann sphere, the northern and southern hemispheres are now equal. To complete the symmetry one also replaces $f(z) - n(z)/d(z)$ by $1/f(z) - d(z)/n(z)$ at such points for the greedy choice of the next support point.

If we make the changes just described, different symmetries are broken, the conditions of translation-invariance and scale-invariance in f of Proposition 3.1. The source of the problem is the constant 1 in the expressions $1/r$, $1/f$, and $|f(z)| > 1$. (On the Riemann sphere, we have privileged the equator over other latitudes.) To restore scale-invariance in f one could replace the condition $|f(z)| > 1$ by $|f(z)| > C$, where C is a constant that scales with f such as the median of the values $|f(Z)|$.

Besides invariance properties and elegance, another reason for imposing a large-small symmetry is to make it possible to treat problems where f takes the value ∞ at some points of Z . For example, this would be necessary in the “ezplot” example of Figure 4.2 if the interval $[-1.5, 1.5]$ were changed to $[-1, 1]$, making -1 into one of the sample points. In the symmetric setting, such a function value is no different from any other.

8. Modified algorithms to impose even, odd, or real symmetry. Many applications involve approximation with a symmetry: f may be an even or an odd function on a set with $Z = -Z$, or f may be hermitian in the sense of satisfying

$f(\bar{z}) = \overline{f(z)}$ on a subset of the real line or some other set with $Z = \bar{Z}$. The core AAA algorithm will usually break such symmetries, with consequences that may be unfortunate in practice and disturbing cosmetically. One may accordingly turn to variants of the algorithm to preserve the symmetries by choosing new support points usually in pairs, two at a time (perhaps with the point $z = 0$ treated specially).

We saw an example of even symmetry in §§6.7 in the approximation of $|x|$ on $[-1, 1]$, where the core AAA algorithm produced unwanted poles. So far as we are aware, such cases of even or odd functions can usually be treated effectively by changing variables from z to $z^{1/2}$ rather than modifying the AAA algorithm.

The case of hermitian symmetry is different in that one can sometimes achieve a superficial symmetry while still not coping with a deeper problem. If $|x|$ is approximated on a set $Z \subseteq [-1, 2]$, for example, then all support points will of course be real and no complex numbers will appear. Nevertheless, there is the problem that the AAA algorithm increases the rational type one at a time, so that odd steps of the iteration, at least, will necessarily have at least one real pole, which will often appear near the singular point $x = 0$. We do not have a solution to offer to this problem.

9. Modified algorithm for approximations of type (μ, ν) . In many applications, as well as theoretical investigations, it is important to consider rational approximations of type (μ, ν) with $\mu \neq \nu$. The barycentric representation (2.5) is still applicable here, with a twist. It is now necessary to restrict the weight vector $\{w_j\}$ to lie in an appropriate subspace in which the numerator degree is constrained to be less than the denominator degree, or vice versa. This concept is familiar in the extreme case of polynomial approximation, $\nu = 0$, where it is well known that the barycentric weights must take a special form [13]. Barycentric representations of type (μ, ν) rational functions are a natural generalization of this case [12, Sec. 3].

Treatment of approximations with $\mu \neq \nu$ raises many issues. The barycentric representations must be generalized as just mentioned, and this adds new linear algebra features to the algorithm. There is also the important practical matter of determining representations with minimal values of ν to achieve various goals. For example, based on boundary values of a meromorphic function on the unit circle, how best can one determine all its poles in the disk? The discussion of §§6.3 indicated some of the challenges here. Algorithms for minimizing the degree of the denominator have been presented for Padé approximation [21] and interpolation in roots of unity [22], and it would be very useful to develop analogous extensions of AAA approximation.

10. Other variants. We have referred to the “core” AAA algorithm to emphasize that in certain contexts, the use of variants would be appropriate. Three of these have been mentioned in the last three sections. We briefly comment here on five further variants.

Weighted norms can be introduced in the least-squares problem at each step by scaling the rows of the matrix $A^{(m)}$ of (3.6). (One may also apply a nonuniform weight in the greedy nonlinear step of the algorithm.) This may be useful in contexts where some regions of the complex plane need to be sampled more finely than others, yet should not have greater weight. For example, we used 200,000 points to get a good approximation of $[-1, 1]$ in the approximation of $|x|$ in Section 6.7, but one can get away with fewer if the points are exponentially graded but with an exponentially graded weight function to compensate.

Continuous sample sets Z such as $[-1, 1]$ or the unit disk are commonly of interest in applications, and while Z is usually discrete in practice, it is very often an approximation to something continuous. But we can also formulate the AAA algorithm in a

continuous setting from the start, with M taking the value ∞ . The barycentric representation (2.5) remains discrete, along with its set of support points, but the selection of the next support point at step m now involves a continuous rather than discrete optimization problem, and the least-squares problem (3.4) is now a continuous one. (Chebfunners say that the Löwner and Cauchy matrices (3.6) and (3.7) become $\infty \times m$ *quasimatrices*, continuous in the vertical direction.) Questions of weighted norms will necessarily arise whenever Z mixes discrete points with continuous components; here the least-squares problem could be defined by a Stieltjes measure.

From an algorithmic point of view, problems with continuous sample sets suggest variants of AAA based on a discrete sample set Z that is enlarged as the computation proceeds. Such an approach is used in [24].

Confluent sample points is the phrase we use to refer to a situation in which one wishes to match certain derivative data as well as function values; one could also speak of “Hermite-AAA” as opposed to “Lagrange-AAA” approximation. Antoulas and Anderson consider such problems in [2], treating them by adding columns such as $(Z_i^{(m)} - z_m)^{-k}$ with $k > 1$ to the Cauchy matrix (3.7) as well as new rows to the Löwner matrix $A^{(m)}$ of (3.6) to impose new conditions. The setting in [2] is interpolatory, so weighting of rows is not an issue except perhaps for numerical stability, but such a modification for us would require a decision about how to weight derivative conditions relative to others.

Another variant is the use of *non-interpolatory approximations*. Here, instead of including free parameters $\{w_j\}$ only in the numerator $n(z)$ of (2.5), which forces $n(z)/d(z)$ to interpolate f at the support points, we allow free parameters in both $n(z)$ and $d(z)$ — say, $\{\alpha_j\}$ and $\{\beta_j\}$. This is a straightforward extension of the least-squares problem (3.4), with each column of the Löwner matrix (3.6) splitting into two, and the result is a rational approximation in barycentric form that does not necessarily interpolate the data at any of the sample points. In such a case (which no longer has much link to Antoulas and Anderson) we are coming closer to the method of fundamental solutions as mentioned in the introduction, though still with the use of the rational barycentric representation (2.5). The sample points and support points can be chosen completely independently. Our experiments suggest that for many applications, non-interpolatory approximants are not so different from interpolatory ones, and they have the disadvantage that computing the SVD of the expanded Löwner matrix takes about four times as long, which can be an issue for problems like Application 6.4 where m is large. (A related issue of speed is the motivation of [11].) However, we now mention at least one context in which the non-interpolatory approach may have significant advantages.

This is the matter of *iterative reweighting*, the basis of the algorithm for minimax approximation known as *Lawson’s algorithm* [17, 27]. Suppose an approximation $r \approx f$ is computed by m steps of the AAA algorithm. Might it then be improved to reduce the maximum error to closer to its minimax value? The Lawson idea is to do such a thing by an iteration in which at each step, least squares weights are multiplied by the corresponding error values at those points. We have explored this idea for barycentric weights and find it shows promise. If the AAA calculation is run in the interpolatory mode, then there is no chance of a true minimax approximation, since half the parameters are used up in enforcing interpolation at prescribed points, so for Lawson iterative reweighting, non-interpolatory approximation seems better. Simple experiments for real functions on an interval produce elegant equioscillatory error curves, and we hope to report on this topic in a future publication.

11. Conclusion. The barycentric representation of rational functions is a flexible and robust tool, enabling all kinds of computations that would be impossible in floating point arithmetic with other representations. All but three of the Cauchy matrices C (3.7) utilized in the examples of this article have condition numbers close to 1, and not greater than 40; the exceptions are the Cauchy matrices for the $\beta = 256$ approximations of Applications 6.3 and 6.4, with $\kappa(C) \approx 10^4$, and for Application 6.8, with its exponentially graded grid, with $\kappa(C) \approx 10^8$. Such anomalies are associated with support points that come very close together.

If the AAA algorithm seems very different from other methods for rational approximation that have been proposed, that is not because it is very advanced, but only because rational barycentric representations have been so little explored. We note that the algorithm makes use of both a linearized residual (for speed of solving a least-squares problem) and a nonlinear one (the measure of ultimate interest in approximation), and further improvements may be achieved by coupling the linear and nonlinear parts together more closely.

We finish with one more example. The following Matlab sequence evaluates the Riemann zeta function at 100 points on the complex line segment from $4 - 40i$ to $4 + 40i$, constructs a AAA approximant r of type $(29, 29)$, and evaluates its poles and zeros. This requires a bit less than a second on our desktop computer:

```
zeta = @(z) sum(bsxfun(@power,(1e5:-1:1)',-z))
[r,pol,res,zer] = aaa(linspace(4-40i,4+40i),zeta)
```

The approximation has a pole at $1.00000000000041 - 0.0000000000066i$ with residue $0.999999999931 - 0.0000000014i$ and a zero at $0.5000000000027 + 14.134725141718i$. These results match numbers for $\zeta(z)$ in each case in all digits but the last two.

Acknowledgements. We thank Anthony Austin, Silviu Filip, and Stefan Güttel for advice at many stages of this project. It was Güttel who pointed us to (6.1).

REFERENCES

- [1] A. C. ANTOUNAS, *Approximation of Large-Scale Dynamical Systems*, SIAM, 2005.
- [2] A. C. ANTOUNAS AND B. D. Q. ANDERSON, On the scalar rational interpolation problem, *IMA J. Math. Contr. Inf.*, 3.2-3 (1986), 61–88.
- [3] A. I. APTEKAREV, *Sharp constants for rational approximations of analytic functions*, Sb. Math. 193 (2002), pp. 1–72.
- [4] A. I. APTEKAREV AND M. L. YATTSELEV, *Padé approximants for functions with branch points—strong asymptotics of Nuttall–Stahl polynomials*, Acta Math. 215 (2015), pp. 217–280.
- [5] A. P. AUSTIN, P. KRAVANJA, AND L. N. TREFETHEN, *Numerical algorithms based on analytic function values at roots of unity*, SIAM J. Numer. Anal., 52 (2014), pp. 1795–1821.
- [6] G. A. BAKER, JR. AND P. GRAVES-MORRIS, *Padé Approximants*, 2nd ed., Cambridge U. Press, 1996.
- [7] A. H. BARNETT AND T. BETCKE, *Stability and convergence of the method of fundamental solutions for Helmholtz problems on analytic domains*, J. Comp. Phys., 227 (2008), pp. 7003–7026.
- [8] B. BECKERMANN, G. LABAHN, AND A. C. MATOS, On rational functions without Froissart doublets, arXiv:1605.00506, 2016.
- [9] V. BELEVITCH, *Interpolation matrices*, Philips Res. Repts. 25 (1970), pp. 337–369.
- [10] J.-P. BERRUT, *Rational functions for guaranteed and experimentally well-conditioned global interpolation*, Comput. Math. Appl., 15 (1988), pp. 1–16.
- [11] J.-P. BERRUT, *A matrix for determining lower complexity barycentric representations of rational interpolants*, Numer. Algs. 24 (2000), pp. 17–29.

- [12] J.-P. BERRUT, R. BALTENSPERGER, AND H. D. MITTELMANN, Recent developments in barycentric rational interpolation, in *Trends and Applications in Constructive Approximation*, 2005, Birkhäuser, pp. 27–51.
- [13] J.-P. BERRUT AND L. N. TREFETHEN, *Barycentric Lagrange interpolation*, SIAM Rev., 46 (2004), pp. 501–517.
- [14] D. BRAESS, *Nonlinear Approximation Theory*, Springer, 1986.
- [15] C. BREZINSKI AND M. REDIVO ZAGLIA, *Extrapolation Methods: Theory and Practice*, v. 2, Elsevier, 2013.
- [16] T. A. DRISCOLL, N. HALE, AND L. N. TREFETHEN, eds., *Chebfun User's Guide*, Pafnuty Publications, Oxford, 2014; see also www.chebfun.org.
- [17] S. ELLACOTT AND J. WILLIAMS, *Rational Chebyshev approximation in the complex plane*, SIAM J. Numer. Anal. 13 (1976), pp. 310–323.
- [18] B. FORNBERG AND N. FLYER, *A Primer on Radial Basis Functions with Applications to the Geosciences*, SIAM, 2015.
- [19] M. FROISSART, *Approximation de Padé: application à la physique des particules élémentaires*, RCP, Programme No. 25, v. 9, CNRS, Strasbourg, 1969, pp. 1–13.
- [20] D. GAIER, *Lectures on Complex Approximation*, Birkhäuser, 1987.
- [21] P. GONNET, S. GÜTTEL, AND L. N. TREFETHEN, *Robust Padé approximation via SVD*, SIAM Rev. 55 (2013), pp. 101–117.
- [22] P. GONNET, R. PACHÓN AND L. N. TREFETHEN, *Robust rational interpolation and least-squares*, Elect. Trans. Numer. Anal., 38 (2011), pp. 146–167.
- [23] S. GÜTTEL AND L. KNIZHNERMAN, *A block-box rational Arnoldi variant for Cauchy–Stieltjes matrices*, BIT Numer. Math. 53 (2013), pp. 595–616.
- [24] S. ITO AND Y. NAKATSUKASA, *Stable polefinding and rational least-squares fitting via eigenvalues*, manuscript, 2016.
- [25] G. KLEIN, *Applications of Linear Barycentric Rational Interpolation*, thesis, U. of Fribourg, 2012.
- [26] A. KLÖCKNER, A. BARNETT, L. GREENGARD, AND M. O'NEIL, *Quadrature by expansion: a new method for the evaluation of layer potentials*, J. Comp. Phys. 252 (2013), pp. 332–349.
- [27] C. L. LAWSON, *Contributions to the Theory of Linear Least Maximum Approximations*, thesis, UCLA, 1961.
- [28] E. LEVIN AND E. B. SAFF, *Potential theoretic tools in polynomial and rational approximation*, in *Harmonic Analysis and Rational Approximation*, Springer, 2006, pp. 71–94.
- [29] D. J. NEWMAN, *Rational approximation to $|x|$* , Mich. Math. J. 11 (1964), pp. 11–14.
- [30] A. V. OPPENHEIM AND R. W. SCHAFER, *Discrete-Time Signal Processing*, Prentice Hall, 2010.
- [31] CH. POMMERENKE, *Padé approximants and convergence in capacity*, J. Math. Anal. Appl., 41 (1973), pp. 775–780.
- [32] H. E. SALZER, *Rational interpolation using incomplete barycentric forms*, Z. Angew. Math. Mech., pp. 61 (1981), pp. 161–164.
- [33] C. SCHNEIDER AND W. WERNER, *Some new aspects of rational interpolation*, Math. Comp., 47 (1986), pp. 285–299.
- [34] O. SÈTE AND J. LIESEN, *Properties and examples of Faber–Walsh polynomials*, Comput. Methods Funct. Theory (2016), pp. 1–27.
- [35] H. STAHL, *Best uniform rational approximation of $|x|$ on $[-1, 1]$* , Russian Acad. Sci. Sb. Math. 76 (1993), pp. 461–487.
- [36] H. STAHL, *The convergence of Padé approximants to functions with branch points*, J. Approx. Th., 91 (1997), pp. 139–204.
- [37] H. STAHL, *Spurious poles in Padé approximation*, J. Comp. Appl. Math., 99 (1998), pp. 511–527.
- [38] L. N. TREFETHEN, *Approximation Theory and Approximation Practice*, SIAM, 2013.
- [39] L. N. TREFETHEN, J. A. C. WEIDEMAN, AND T. SCHMELZER, *Talbot quadratures and rational approximations*, BIT Numer. Math. 43 (2006), 653–670.
- [40] R. S. VARGA AND A. J. CARPENTER, *On the Bernstein conjecture in approximation theory*, Constr. Approx. 1 (1985), pp. 333–348.
- [41] J. L. WALSH, *Interpolation and Approximation by Rational Functions in the Complex Domain*, 5th ed., Amer. Math. Soc., 1969.
- [42] E. WEGERT, *Visual Complex Functions: An Introduction with Phase Portraits*, Birkhäuser, 2012.